Low-frequency electric microfield distributions in plasmas

Carlos A. Iglesias and Hugh E. DeWitt
Lawrence Livermore National Laboratory, University of California, Livermore, California 94550

Joel L. Lebowitz and David MacGowan
Department of Mathematics and Physics, Rutgers University, New Brunswick, New Jersey 08903

William B. Hubbard
Department of Planetary Sciences, University of Arizona, Tucson, Arizona 87521

(Received 1 October 1984)

We evaluate the low-frequency component electric microfield distribution at a charged point, i.e., the field distribution due to ions, possibly of different species, which interact through an electron-screened potential. The method employed is an adaptation of the adjustable-parameter exponential (APEX) approximation previously developed for the high-frequency component and involves a noninteracting-quasiparticle representation of the electron-screened ions designed to yield the correct second moment of the microfield distribution. The APEX results are compared to Monte Carlo simulations, and we find good agreement.

I. INTRODUCTION

The profiles of spectral lines emitted by atoms and ions immersed in a plasma provide diagnostic tools for inferring the state of plasma.[1] For a wide class of spectral lines, the observed frequencies (measured from line center) are sufficiently large that the ions in the plasma are effectively stationary over the corresponding radiation times. Consequently, the perturbing ions may be treated by the statistical broadening theories of Holtsmark[2] and Margenau.[3] The basic picture in this theory is that the radiator finds itself in a statistically fluctuating electric field produced by the configurations of the perturbing ions. Thus, the problem is reduced to determining the probability distribution of the perturbing electric field.

Recently a method was proposed for calculating electric microfield distributions which provides numerical results in excellent agreement with computer simulations for strongly coupled plasmas.[4–6] In these works the plasma consisted of point charges moving in a uniform neutralizing background which models the high-frequency component of the field.[7,8] However, spectral line calculations primarily require the so-called low-frequency component distribution.[7–9] The latter is approximately determined by considering a gas of ions interacting through electron screened potentials. The electron screening of the ions is a way to incorporate into the statistical broadening theory the total static electric field at the radiator due to the plasma;[10] that is, it includes static contributions from both ions and electrons.

The objective of this note is to extend the "adjustable-parameter exponential" (APEX) approximation to the low-frequency component microfield distribution in ion mixtures. The model for the low-frequency component distribution is described in Sec. II, followed by a statement of the second-moment condition. The necessary modifications of APEX are presented in Sec. III. Numerical results are compared with Monte Carlo simulations and other approximate theories in Sec. IV. Concluding remarks are given in Sec. V.

II. LOW-FREQUENCY COMPONENT

We consider the electric microfield distribution $W(\epsilon)$, defined as the probability density of finding a field $\mathbf{E}$ equal to ϵ at an ion of charge $Z_0 e$, located at $\mathbf{r}_0$, due to an ionic mixture where ions of species σ carry a charge $Z_\sigma e$. Here, e is the magnitude of the elementary charge and Z_0 and all the Z_σ's are positive. As usual,[7,8] we assume that the electron screening is described by a Debye-Hückel formula.[11] This can be justified only for plasma conditions such that the electron-electron and electron-ion coupling are both weak and the plasma may be described by classical mechanics.[12] For situations where these conditions are not met, more realistic screened potentials have been proposed in recent papers by Rogers[13] and Dharma-Wardana, *et al.*[14]

The system is assumed to be described by classical equilibrium statistical mechanics with temperature T and number densities ρ_σ,

$$\rho_\sigma = N_\sigma/\Omega \text{ and } N=\sum_\sigma N_\sigma \ , \tag{2.1}$$

where N_σ is the number of ions of species σ, N the total number of ions, and Ω the total volume. We have then, in the limit of a macroscopic system,

$$W(\epsilon)=\langle \delta(\epsilon-\mathbf{E})\rangle = \int\cdots\int d\mathbf{r}_0 \prod_{j=1}^{N} d\mathbf{r}_j \frac{e^{-\beta V}\delta(\epsilon-\mathbf{E})}{Q(\{N_\sigma\},\Omega,T)} \ , \tag{2.2}$$

where $Q(\{N_\sigma\},\Omega,T)$ is the configurational partition function, $\mathbf{r}_j$ the position of the jth ion, and $\beta=(k_B T)^{-1}$. For notational convenience the thermodynamic limit, i.e., $\{N_\sigma\}$ and Ω tend to infinity with $\{\rho_\sigma\}$ fixed, has not been

explicitly specified. The potential energy V is given by

$$V=V_0+V_p\ , \tag{2.3}$$

where V_0 describes the interaction between the ionic mixture and the charge at $\mathbf{r}_0$,

$$V_0=\sum_{j=1}^{N}\frac{Z_0Z_{\sigma_j}e^2}{|\mathbf{r}_0-\mathbf{r}_j|}\exp(-\kappa|\mathbf{r}_0-\mathbf{r}_j|)\ , \tag{2.4}$$

V_p describes the interaction between the ions in the mixture

$$V_p=\sum_{1\le i<j\le N}\frac{Z_{\sigma_i}Z_{\sigma_j}e^2}{|\mathbf{r}_i-\mathbf{r}_j|}\exp(-\kappa|\mathbf{r}_i-\mathbf{r}_j|)\ , \tag{2.5}$$

and σ_j denotes the species of the jth ion. The quantity κ appearing in Eqs. (2.4) and (2.5) is the inverse Debye length for electrons

$$\kappa^2=4\pi e^2\beta\rho_e \tag{2.6}$$

with ρ_e the electron number density. The total system is required to be neutral so that

$$\rho_e=\sum_\sigma Z_\sigma\rho_\sigma\ . \tag{2.7}$$

The electron-screened ion electric field at $\mathbf{r}_0$ is given by

$$\mathbf{E}=\sum_{j=1}^{N}Z_{\sigma_j}ef(|\mathbf{r}_0-\mathbf{r}_j|)(\mathbf{r}_0-\mathbf{r}_j)\Big/|\mathbf{r}_0-\mathbf{r}_j|\ , \tag{2.8}$$

where

$$f(r)=\frac{1}{r^2}(1+\kappa r)\exp(-\kappa r)\ . \tag{2.9}$$

It is convenient to introduce the Fourier transform of the distribution $W(\epsilon)$. In the thermodynamic limit the system is isotropic, so that after setting $\epsilon=|\epsilon|$,

$$P(\epsilon)=4\pi\epsilon^2W(\epsilon)=\frac{2\epsilon}{\pi}\int_0^\infty dk\,k\sin(k\epsilon)T(k)\ , \tag{2.10}$$

where

$$T(k)=\langle\exp(i\mathbf{k}\cdot\mathbf{E})\rangle\ . \tag{2.11}$$

We now consider the second moment of the distribution $W(\epsilon)$. For the high-frequency component, the second moment is given explicitly[4–6] by a simple expression involving the charges, temperature, and set of densities $\{\rho_\sigma\}$. Unfortunately, no such simple result holds for the low-frequency component. Instead, the second moment may be determined from the radial distribution functions which themselves are only known approximately but are much easier to calculate than $W(\epsilon)$.

Following the procedure in Ref. 4, we write

$$\begin{aligned}\langle\mathbf{E}\cdot\mathbf{E}\rangle&=(Z_0e)^{-2}\langle\nabla_0V\cdot\nabla_0V\rangle\\&=(Z_0^2e^2\beta)^{-1}\langle\nabla_0^2V\rangle\ ,\end{aligned} \tag{2.12}$$

where ∇_0 is the gradient with respect to $\mathbf{r}_0$. Substituting Eqs. (2.3)–(2.5) into Eq. (2.12) yields

$$\begin{aligned}\langle\mathbf{E}\cdot\mathbf{E}\rangle&=(Z_0^2e^2\beta)^{-1}\left\langle\kappa^2V_0-4\pi Z_0e^2\sum_{j=1}^{N}Z_{\sigma_j}\delta(\mathbf{r}_0-\mathbf{r}_j)\right\rangle\\&=\frac{4\pi}{\beta Z_0}\sum_\sigma Z_\sigma\rho_\sigma\psi_\sigma(\kappa)\ ,\end{aligned} \tag{2.13}$$

where

$$\psi_\sigma(\kappa)=\kappa^2\int_0^\infty dr\,rg_\sigma(r)\exp(-\kappa r) \tag{2.14}$$

and $g_\sigma(r)$ denotes the distribution of ions of species σ a distance r from the charge Z_0e. In obtaining Eq. (2.13) we used the fact that the delta functions only contribute when the positions of the two particles coincide, which has zero probability. We remark that the expression in Eq. (2.13) is the high-frequency result modified by the factor $\psi_\sigma(\kappa)$ which has the property

$$\lim_{\kappa\to0}\psi_\sigma(\kappa)=1+O(\kappa^2)\ , \tag{2.15}$$

and therefore, Eq. (2.13) reduces to the high-frequency result[4,5] in the limit of no screening.

III. MODIFICATIONS OF APEX

The method presented in this section is based on the APEX formalism developed in Refs. 4 and 5. We indicate the modifications necessary to apply that theory to the low-frequency component distribution.

The original formulation of APEX[4] involved replacing a one-component plasma by a system of noninteracting quasiparticle, each producing a parametrized electric field at the charge Z_0e. The quasiparticles had a distribution about $\mathbf{r}_0$, which was different from that of the fully interacting point charges, and was determined by satisfying a "local-field constraint": The field produced at $\mathbf{r}_0$ by the quasiparticles contained in a volume element $d\mathbf{r}$ located at $\mathbf{r}$ must be equal to the field produced by the interacting point charges contained in the same $d\mathbf{r}$ for all $\mathbf{r}$.

The extension of APEX to ionic mixtures with bare Coulomb interactions in a uniform neutralizing background introduced a parameter set $\{\alpha_\sigma\}$ (one parameter per species) characterizing the quasiparticle fields.[5] In order to solve for the $\{\alpha_\sigma\}$ and the quasiparticle distribution about $\mathbf{r}_0$, it was assumed that both the second-moment sum rule and local-field constraint were valid species by

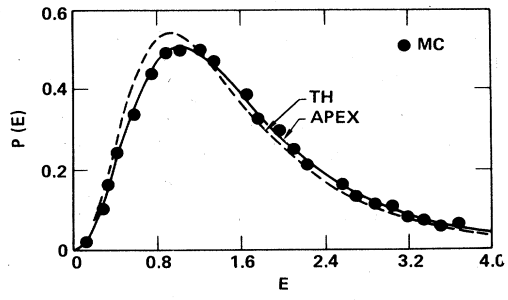

FIG. 1. Comparison of $P(\epsilon)$ curves in units defined in Eq. (4.1) for plasma with a single-ion species of charge $Z_0=Z_1=9$ and $\Gamma_e=0.053$.

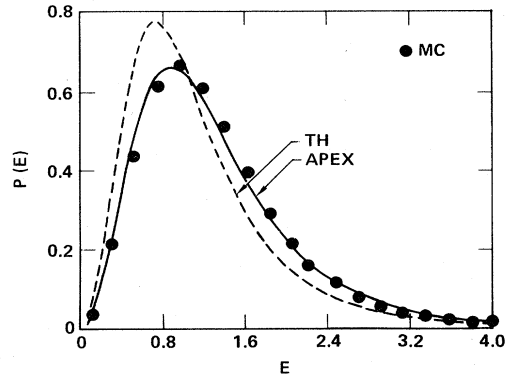

FIG. 2. Same as Fig. 1 with $Z_0=Z_1=17$ and $\Gamma_e=0.053$.

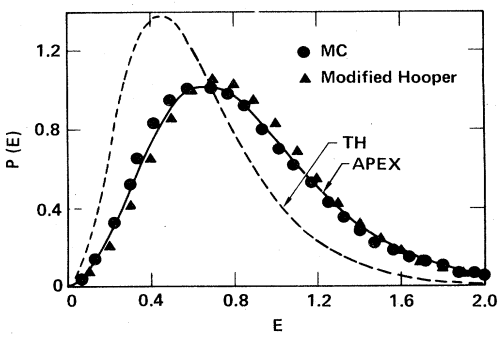

FIG. 3. Same as Fig. 1 with $Z_0=Z_1=35$ and $\Gamma_e=0.053$.

species. Here, we follow the same procedure but with modifications due to the electron screening of the ion-ion interactions.

Let us now introduce the quantities $G_\sigma(r)$ and $Z_\sigma eF_\sigma(r)$ which denote the distribution of quasiparticles of species σ, a distance r from the charge Z_0e, and the magnitude of the electric field at $\mathbf{r}_0$ due to one such quasiparticle, respectively. Assuming that the local-field constraint is valid species by species, then we have

$$\rho_\sigma G_\sigma(r)Z_\sigma eF_\sigma(r)\,d\mathbf{r}=\rho_\sigma g_\sigma Z_\sigma ef(r)\,d\mathbf{r}\ , \tag{3.1}$$

or equivalently,

$$G_\sigma(r)=g_\sigma(r)f(r)/F_\sigma(r)\ , \tag{3.2}$$

for all σ. The choice for $F_\sigma(r)$ is a parametrized Debye field,[4–6]

$$F_\sigma(r)=\frac{(1+\alpha_\sigma r)}{r^2}\exp(-\alpha_\sigma r)\ . \tag{3.3}$$

The noninteracting quasiparticle picture together with the distributions $G_\sigma(r)$ in Eq. (3.2) may be used to obtain the expression,

$$T(k)=\exp\left[4\pi\sum_\sigma\rho_\sigma\int_0^\infty dr\,r^2g_\sigma(r)\frac{f(r)}{F_\sigma(r)}\{j_0[kZ_\sigma eF_\sigma(r)]-1\}\right]\ , \tag{3.4}$$

where j_0 is the spherical Bessel function of order zero.

Values for the parameters $\{\alpha_\sigma\}$ are obtained by comparing the second-moment expression from Eqs. (2.13) and (3.4),

$$\sum_\sigma Z_\sigma^2\rho_\sigma e^2\int_0^\infty dr\,r^2g_\sigma(r)f(r)F_\sigma(r) = \sum_\sigma Z_\sigma\rho_\sigma\psi_\sigma(\kappa)\Big/\beta Z_0 \tag{3.5}$$

which if assumed valid species by species leads to

$$Z_0Z_\sigma\beta e^2\int_0^\infty dr\,r^2g_\sigma(r)f(r)F_\sigma(r)=\psi_\sigma(\kappa). \tag{3.6}$$

Equation (3.6) together with knowledge of the distributions $g_\sigma(r)$ provide a scheme for evaluating the parameter set $\{\alpha_\sigma\}$ and hence the low-frequency component microfield distribution.

IV. NUMERICAL RESULTS

For simplicity, we restrict the calculations to plasmas with either one or two ion species. Also, the results are limited to cases where Z_0 is set equal to one of the plasma ion charges since computer simulations are impractical otherwise. The required radial distribution functions were evaluated in the hypernetted-chain approximation generalized to multicomponent plasmas.[15] The plots presented are for $P(\epsilon)$ versus ϵ with the electric field in units of ϵ_0,

$$\epsilon_0=e/a_e^2\ , \tag{4.1}$$

where a_e is the electron sphere radius

$$\frac{4\pi}{3}\rho_e a_e^3=1\ . \tag{4.2}$$

The plasma state is defined by the electron coupling parameter

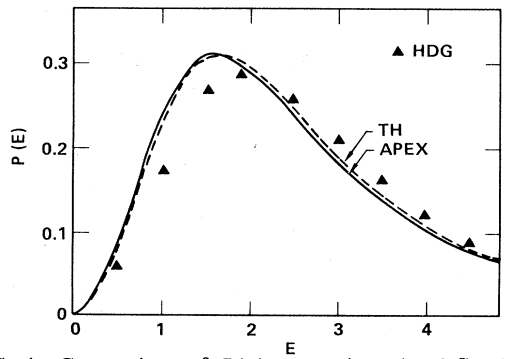

FIG. 4. Comparison of $P(\epsilon)$ curves in units defined in Eq. (4.1) for a binary mixture with charges $Z_0=Z_1=9$ and $Z_2=1$, number fractions $x_1=x_2=0.50$, and $\Gamma_e=0.013$.

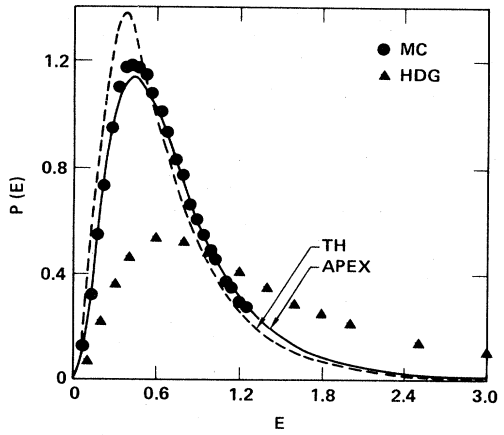

FIG. 5. Same as Fig. 4 with $Z_0=Z_1=9$ and $Z_2=1$, $x_1=x_2=0.50$, and $\Gamma_e=0.21$.

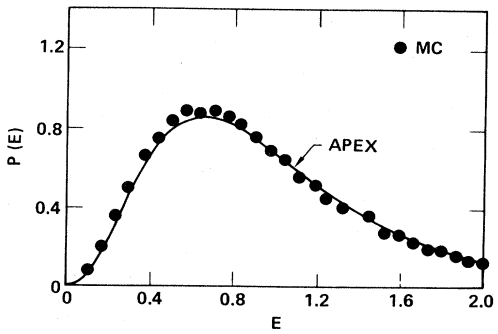

FIG. 6. Same as Fig. 4 with $Z_0=Z_1=17$ and $Z_2=1$, $x_1=x_2=0.50$, and $\Gamma_e=0.13$.

$$\Gamma_e=\beta e^2/a_e \tag{4.3}$$

along with the sets $\{Z_\sigma\}$ and $\{x_\sigma\}$, where x_σ is the number fraction for species σ,

$$x_\sigma=N_\sigma/N\ . \tag{4.4}$$

In Figs. 1—3 the APEX results are presented for plasmas with a single-ion species. These are compared with Monte Carlo (MC) data and the results of Tighe and Hooper (TH).[16] It is important to note that in Figs. 2 and 3 the so-called α plateau of the Hooper formalism is not well defined.[17] This has been interpreted as a lack of self-consistency in the Hooper method and indicates an application of that method outside its range of validity.[8]

In an attempt to extend the reliability of the Tighe and Hooper calculations, the free parameter in that theory was selected to satisfy the second-moment condition and the results are presented in Fig. 3 (modified Hooper). It is clear from the figure that the second-moment constraint greatly improves their agreement with Monte Carlo data, an indication of the importance exact-moment relations have in computing microfield distributions.

In Figs. 4—6 the APEX results are given for plasmas with two ionic species. These are compared with MC data except in Fig. 4 where the plasma is too weakly coupled for computer simulations to be reliable. In that figure the comparison is the TH and recent calculations by Held *et al.* (HDG).[18] Although the three theories agree in the Debye-Hückel limit,[4,18] for the plasma conditions of Fig. 4 only APEX and TH are in close agreement. For more strongly coupled plasmas, as in Fig. 5, neither TH nor HDG are in agreement with APEX which, however, is in good agreement with MC data. As in Figs. 2 and 3, the TH results in Fig. 5 are known to be outside their range of validity.

V. CONCLUSION

The simple APEX method, although phenomenological and based on an independent quasiparticle model, has been shown to provide results in excellent agreement with computer simulations for both high-[4,5] and low-frequency component distributions. The reasons for its success are not entirely clear but it is possible to give a partially satisfactory *a posteriori* justification. For small fields the contributions from many ions are important and these are well characterized by the second moment of the microfield distribution which is exactly included in APEX through Eq. (3.6). On the other hand, large fields are predominantly caused by a single ion near the test charge and such a situation is accurately described by an independent particle model.

It should be emphasized that the cluster expansions[7,8,16,18] also contain single-particle contributions, for example, the first term in the Baranger-Mozer series. However, in APEX many-body effects are included by introducing the screened quasiparticle fields (fields are only partially screened in the Hooper formalism[8,16] and not at all in the Baranger-Mozer methods).[7,18] Furthermore, the quasiparticle distributions in APEX are modified through the local-field constraint in Eq. (3.1). This latter constraint is numerically important (see Fig. 3 and Ref. 4) and physically plausible. Its apparent effect is to extend the single-particle picture toward intermediate field values by imposing a self-consistency condition between the screened electric field and density distribution of the quasiparticles.

ACKNOWLEDGMENTS

The authors are grateful to F. J. Rogers for his multicomponent hypernetted-chain computer program. We also thank C. F. Hooper and L. A. Woltz for providing us with the numerical results of the Hooper *et al.* calculations. The work at Rutgers was supported in part by the U.S. Air Force Office of Scientific Research Grant No. 82-0016 and the work at Livermore by contracts from the U.S. Department of Energy by Lawrence Livermore National Laboratory under Contract No. W-7405-Eng-48. The work of H.E. DeWitt is also supported by the Office of Naval Research.

[1]For example, D. Mihalas, *Stellar Atmospheres* (Freeman, San Francisco, 1978).
[2]J. Holtsmark, Ann. Phys. (Leipzig) **58**, 577 (1919).
[3]H. Margenau and M. Lewis, Rev. Mod. Phys. **31**, 569 (1959).
[4]C. A. Iglesias, J. L. Lebowitz, and D. MacGowan, Phys. Rev. A **28**, 1667 (1983); The second-moment result for the one-component plasma is implicit in the article by J. P. Hansen, *Strongly Coupled Plasmas,* edited by G. Kalman (Plenum, New York, 1978), p. 133.
[5]C. A. Iglesias and J. L. Lebowitz, Phys. Rev. A **30**, 2001 (1984).
[6]A. Alastuey, C. A. Iglesias, J. L. Lebowitz, and D. Levesque, Phys. Rev. A **30**, 2537 (1984).
[7]M. Baranger, and B. Mozer, Phys. Rev. **115**, 521 (1959); B. Mozer and M. Baranger, *ibid.* **118**, 626 (1960).
[8]C. F. Hooper, Jr., Phys. Rev. **149**, 177 (1966); **165**, 21 (1968).
[9]H. Griem, *Spectral Line Broadening by Plasmas* (Academic, New York, 1974).
[10]C. A. Iglesias and J. W. Dufty, in *Spectral Line Shapes II,* edited by K. Burnett (Walter de Gruyter, Berlin, 1983), p. 55; C. A. Iglesias, Phys. Rev. A **29**, 1366 (1984).
[11]P. Debye and E. Hückel, Z. Phys. **24**, 185 (1923).
[12]Quantum effects in electron screening have been considered in C. A. Iglesias and C. F. Hooper, Jr., Phys. Rev. A **25**, 1632 (1982).
[13]F. J. Rogers, Phys. Rev. A **29**, 868 (1984).
[14]M. W. C. Dharma-Wardana, F. Perrot, and G. C. Aers, Phys. Rev. A **28**, 344 (1983).
[15]F. J. Rogers, J. Chem. Phys. **73**, 6272 (1980).
[16]R. J. Tighe and C. F. Hooper, Jr., Phys. Rev. A **15**, 1773 (1977).
[17]L. Woltz and C. F. Hooper (private communication).
[18]B. Held, C. Deutsch, and M.-M. Gombert, Phys. Rev. A **29**, 880 (1984).